Design Study of a Short-Range Airborne UAV Radar for Human Monitoring

Sevgi Zübeyde Gürbüz[1], Ünver Kaynak[2], Bertan Özkan[2], Ozan Can Kocaman[2], Fırat Kıyıcı,[2] Bürkan Tekeli[1]
[1]TOBB University of Economics and Technology, Dept. of Electrical and Electronics Engineering, Ankara, Turkey
[2]TOBB University of Economics and Technology, Dept. of Mechanical Engineering, Ankara, Turkey
szgurbuz@etu.edu.tr, ukaynak@etu.edu.tr, ozkanbertan@gmail.com,
ozan.kocaman1011@gmail.com, firat.kiyici1@gmail.com, btekeli@etu.edu.tr

***Abstract*—Unmanned Aerial Vehicles (UAVs) have many attributes making them advantageous in many surveillance applications, especially the control of borders against illegal trafficking. UAVs are less expensive than conventional aircraft, possess greater maneuverability, and are remotely-operated by its pilot/or autopilot. An important task in border control, however, is to be able to detect and monitor the activities of any people in the region. In particular, discrimination between friendly and non-cooperative targets is of high importance. Over recent years, micro-Doppler analysis has come to the forefront of research as a means to identify not just human targets, but recognize activities as well, using ground-based radar. This work studies the top-level design and tradeoffs involved in the development of a short-range UAV for human monitoring, such as power and weight requirements, frequency and type of radar and signal processing algorithms. As a case study, the performance attainable of a lightweight radar similar to IMSAR's NanoSAR-C with the TAN100 UAV for a human monitoring mission is analyzed.**

I. SUMMARY

Over the years, unmanned aerial vehicles (UAVs) have shown themselves to be useful for a variety of surveillance applications. Generally, UAVs are less expensive than conventional aircraft, possess greater maneuverability, and are remotely-operated by its auto/pilot. As a result, UAVs have also become a unique asset for border control against illegal trafficking. In this regard, the ability to detect and monitor the activities of people, as well as discriminate friendly and non-cooperative targets is of high importance.

Recent research has shown that a target's micro-Doppler signature can be used to discriminate a variety of types of targets [1-2] and even identify several different types of human activities [3-4]. Micro-Doppler is the frequency modulations that appear about the main Doppler shift of a target. They are caused by any rotations or vibrations that are experienced in addition to the target's gross translational motion. Thus, the rotating wheels of a vehicle and spinning of a helicopter blade all result in micro-Doppler. In humans, the oscillatory motion of the arms, legs, and body also result in micro-Doppler. In fact, the pattern observed in micro-Doppler signatures are so unique that it can be used to differentiate humans from animals [5-6], and even whether a person is walking, running, or crawling [7].

However, small radar cross section (RCS) as well as low velocity tends to make both humans and animals easily masked by ground clutter and rather difficult to detect. Moreover, high classification performance also requires a clean micro-Doppler signature of sufficient signal-to noise ratio (SNR). On the other hand, increasing transmitter power and antenna gain also tends to increase the size and weight of the radar hardware, two factors critically impacting the aerodynamic performance of the UAV, such as altitude, range, wingspan, and motor power.

One of the most lightweight, commercially available synthetic aperture radar (SAR) systems is the NanoSAR-C, designed and produced by IMSAR [8]. The nanoSAR-C system is an X-band radar operating at about 10 GHz with a transmitter power of 1 W. Consuming about 30W power, it weights just 2 lb. NanoSAR-C has a range of at most 3 km and adjustable range resolution between 0.3 m and 10 m. Its antenna has a beam width of 45° in elevation and 10° in azimuth.

In this work, the suitability of a NanoSAR-C type small, lightweight radar mounted upon the TAN100 UAV is considered for application to human monitoring missions. Potential performance is analyzed in terms of human detection range and classification rates. Based on results, viability of the TAN100 UAV for carrying SAR systems is demonstrated and modifications to on-board SAR system parameters are evaluated.

II. THE TAN100 ELECTRICAL UAV

The TAN100 UAV was designed and built by TK3-Teknik Inc., a company based in Ankara, Turkey as an unmanned aerial research vehicle [9]. Its design concept assumes a "solar assisted" electrical vehicle, which draws a majority of its energy from a lithium based battery pack that is also charged inflight by wing mounted solar cells during day time. Keeping pace with developing battery storage

capacities and solar cell efficiencies, the reseach vehicle has significant potential to increase its total flight endurance and solar assist part of the energy balanced by the payload weight and cost of high tech solar cells. TAN100 aircraft is pictured in Figure 1.

Figure 1. TAN 100 UAV

Possessing a wingspan of 5 meters, wing area of 2 m^2 and a length of 3 meters, the air vehicle has a cruise speed of 90 km/hr (25 m/s) at an average cruise altitude of 1000 meters. TAN100 uses a low cost commercial autopilot for GPS navigation within close ranges limited by national civil aviation rules. Standard configuration presently includes a mix of Li-Po and Li-Ion batteries (200 W.kg and 240 W.h/kg. respectively) and %13 efficient commercial low cost solar cells. For a typical low maximum take-off weight (Wo=15 kg.) configuration for a short range mission of 2 hours, roughly %30 of the electrical energy is supplied by the solar cells. Based on budget limits, potential use of Li-S batteries (500 W.h/kg), with the expectation of their commercialization, and use of satellite grade solar cells (%35 efficiency), the same mission could be flown with significantly increased flight times and solar energy assist ratios.

TAN100 design philosophy also aims for providing a sufficiently large fuselage bay that allows for experimenting different electrical and electronics equipment with ease of installation and minimum interchange time. Therefore, the vehicle was not shape optimized for a classical total solar flight time criterium but for an increased solar assisted flight to extend the battery-only flight time, as well as to help support the avionics equipment energy needed. To this end, meeting the sufficient weight, volume and energy requirements of different equipment, TAN100 can be missionized to carry a range of miniture sensor payloads including electro-optical sensors and radars.

A particularly interesting situation is the advent of commercially available miniture synthetic aperture radar (SAR) systems. Miniture systems enabled UAVs to carry such valuable payloads, that were otherwise impossible to be carried, thanks to their low weight and virtually diminishing power consumption. This is especially very advantageous for electrically driven UAVs with the ability to use short stand-off distances for better resolution, but having very low acoustic noise signature for low detectability [10]. To demonstrate the viability of the TAN100 to use such payloads, a mission weight, speed and power simulation is conducted for the NanoSAR-C system that was designed and produced by IMSAR [8]. In the simulation, the aircraft is flown without solar cells (for a night mission) but only using Li-S battery pack and using the NanoSAR-C from a maximum stand-off range of 1000 m. The vehicle is flown at a design lift coefficient and constant pitch attitude to provide a stable platform for the radar payload. In the simulation, while progressively changing the design take-off weight (Wo), corresponding airspeed and total required power (sum of flight and sensor power) are calculated. Required battery weights and flight endurance times can then be calculated from the total required power using the battery specific energy level (W.h/kg) of the particular battery in use. Results of such simulation is shown in Table I below.

Table 1.

Wo (kg)	V (m/s)	Preq (W)	Wb (kg)	E (hr)
15	21,0	313	2,1	3,1
16	21,7	344	3,1	4,2
17	22,3	377	4,1	5,0
18	23,0	411	5,1	5,9
19	23,6	446	6,1	6,5
20	24,2	481	7,1	7,0
21	24,8	518	8,1	7,5
22	25,4	555	9,1	7,8

In the simulation, empty weight (We) of the TAN100 was taken to be 12 kg., NanoSAR-C weight and power consumption are 2 lbs. and 30 W respectively. Specific energy of the Li-S battery is taken to be 500 W.h/kg. While the real field data in the future may be expected to be less optimistic, presently run fictitious mission data show that TAN100 is a viable platform to carry NanoSAR-C payload for elongated periods of time. For instance, the shortest time mission configuration uses a Wb = 2.1 kg. of battery weight resulting in a Wo = 15 kg. of design take-off weight, while requiring only Preq= 313 W of total power to propel the aircraft at a speed of V=21 m/s (76 km/hr). Here, the resulting endurance time of E = 3 hours is quite suitable for many tactical missions. As will be shown shortly in the following figures, this airseed also provides quite a good detection range of 850 m. for a 20 m. range resolution (see Fig. 2). With the expense of diminishing detection range, much longer endurance can be obtained by TAN100 by loading larger battery packs. For instance, loading a Wb =7.1 kg of battery pack, the endurance can be extended to as long as E = 7 hours. Meanwhile, the vehicle flight speed will be around V = 24 m/s (86 km/h) with slightly lesser detection range and requiring roughly Wreq = 0.5 kW of battery power. Therefore, once the tactical mission requirements are given by the user, TAN100 aircraft can provide for optimal values of detection range and flight endurance time combinations.

III. HUMAN DETECTION PERFORMANCE

For a coherent detector assuming unknown phase [11], the probability of detection, P_D, may be expressed in terms of SNR and probability of false alarm, P_{FA} as

$$P_D = Q_M\left(\sqrt{2\cdot SNR}, \sqrt{-2\ln(P_{FA})}\right), \quad (1)$$

From (1), a detection probability of 0.9 with a false alarm rate of 10^{-6} requires an SNR of 13 dB. With coherent integration over N pulses, this amounts to a single-pulse SNR of $10\log_{10}(20/N)$ in dB. The single-pulse SNR received by the radar is computable from the range equation:

$$SNR = \frac{P_t G^2 \lambda^2 \sigma}{(4\pi)^3 R^4 kT\beta F_n L_s L_a}, \quad (2)$$

where P_t is the transmit power, G is the antenna gain, λ is the signal wavelength, R is the target range, k is the Boltzmann's constant, T is the standard temperature in Kelvin, β is the receiver bandwidth, L_s is the system loss, and L_a is the atmospheric loss. The atmospheric losses incurred is dependent upon a number of factors, primarily transmit frequency, weather conditions, and range. An estimate of the atmospheric losses may be found using the relation [11]

$$L_a(R) = \frac{\alpha R_{rt}}{500} \text{ in dB}, \quad (3)$$

where α is a loss factor dependent upon frequency and heaviness of precipitation. For medium to heavy rain and an X-band radar, α = 0.01 dB/km. The round-trip distance, R_{rt}, is twice the target range, and for targets at most 20 km away (3) may be used to find that losses are at most 0.8 dB. In this work, we assume system losses are approximately 4 dB and that the noise figure is roughly 5 dB.

Grouping constant parameters into a single constant, A, (2) may be simplified to

$$\frac{20}{N} = \frac{A}{R^4\beta}. \quad (4)$$

The receiver bandwidth should be at least as wide as the transmitted signal bandwidth, which is also a key determinant of range resolution. For pulse compression systems, the range resolution $\Delta R = c / 2\beta$, where c is the speed of light. The greater the bandwidth, the better (the lower) the range resolution – but to the detriment of received SNR.

The radar mode of operation may also place a constraint on the maximum number of pulses that may be coherently integrated in the radar. For a radar operating in stripmap mode, the total time-on-target is limited by the velocity of the aircraft (v), range, azimuthal antenna beam width (θ), and pulse repetition interval (PRI):

$$\frac{R\theta}{v} = N \cdot PRI\ . \quad (5)$$

Thus, while increasing the number of coherently integrated pulses can lower the single-pulse SNR requirement – thereby increasing detection range – the number of pulses is limited by the total time-on-target, which is also a function of range. Figure 2 graphically illustrates these relationships. As the velocity of the aircraft decreases, the time-on-target increases, thereby improving the detection range. The minimum flight velocity for the TAN100 is 18 m/s; thus, for 20 m range resolution the maximum detection range is about 850 m. If a higher range resolution is desired, the detection range drops to just 300 m for 1 m range resolution.

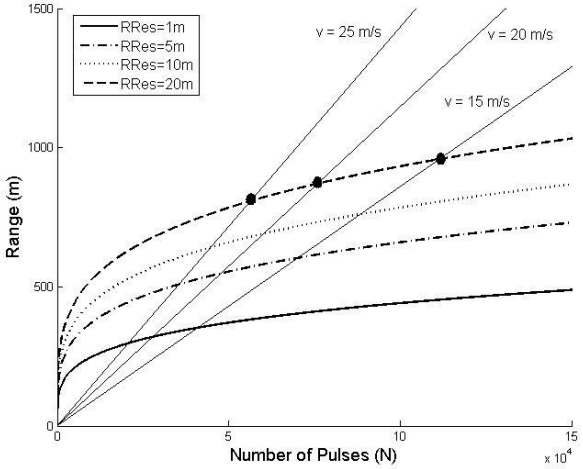

Figure 2. Radar range equation curves illustrating the relationship between pulse number and range for different range resolutions. Limitation on pulse number shown for several different platform velocities.

IV. TARGET CLASSIFICATION PERFORMANCE

Once potential targets are detected, a key operational capability is to be able to identify the target. In border control and security applications, a critical issue is the discrimination of people from animals, especially those often seen in rural areas, such as horses, donkeys, cattle, sheep, and dogs. A unique biological discriminator is the micro-Doppler signatures of targets.

A. Micro-Doppler Signature Simulation

In this work, micro-Doppler signatures for a variety of targets and activities were generated by exploiting video motion capture (MOCAP) data. The methodology for simulating radar micro-Doppler signatures using MOCAP data was first put forth by S.S. Ram, et.al in 2008 [12], as a natural extention of kinematic walking model-based simulations developed by Van Dorp and Groen in 2003 [13]. Recently, it was also shown by Erol, et. al. that less accurate range data acquired by the Kinect sensor could also be used

to simulate micro-Doppler signatures and classify human activities [14].

Often exploited by the movie industry to generate fantastic computer animations, many motion capture databases are freely accessible online [15-18], and contain not just recordings of different activities for many different subjects, but also animal recordings. Highly accurate motion capture data can be acquired by placing infrared cameras on a test subject, and mapping the time-varying locations measured to a 3-dimensional model that incorporates critical joints and muscles of the human body. Thus, MOCAP-based signature simulation is not limited to just walking, but can be used for any recordable activity. Moreover, MOCAP also captures the individual nuances of subject gait as well, leading to statistically variable datasets.

Simulated micro-Doppler signatures are generated from MOCAP data by first modeling various body parts as a point target, using MOCAP measurements to define the time-varying range of each body part, R_i. For a linear frequency modulated pulse-Doppler radar, the expected return is just a time-delayed, frequency shifted copy of the transmitted signal. Adding the returns from each point target to compute the total return from the target,

$$s_h(N,t) = \sum_{i=1}^{K} a_{t,i}\, rect\left(\frac{\hat{t} - t_{d,i}}{\tau}\right) e^{j[-2\pi f_c t_{d,i} + \pi\gamma(\hat{t}-t_{d,i})^2]}, \quad (6)$$

where K is total number of point targets; the time t is defined as $t = T(n-1) + \hat{t}$ in terms of the pulse repetition interval (PRI), T, pulse number, N, and time relative to the start of each PRI, $\hat{t}$; $a_{t,i}$ is the amplitude as given by the radar range equation; τ is the pulse width; c is the speed of light; γ is the chirp slope; f_c is the transmitted center frequency; and $t_{d,i}$ is the round-trip time delay from antenna and point target, defined in terms of the range, R_i, as $t_{d,i} = 2R_i/c$.

The received return computed from (6) is then stored as a slow-time, fast-time data matrix, and pulse compressed so that the peak occurs at the range bin in which the target is present. Taking a slice across slow-time at the range bin of the peak output,

$$x_p[n] = \sum_{i=1}^{12} a_{t,i}\pi e^{-j\frac{4\pi f_c}{c}R_i}, \quad (7)$$

The signal x_p represents the starting point for time-frequency analysis of the return signal.

Although many different time-frequency representations have been used in the literature, the most common representation of micro-Doppler signatures is the spectrogram, which is obtained by taking the magnitude square of the short-time Fourier Transform of the slow-time slice x_p. Example simulated micro-Doppler signatures for a horse, dog, and varying human activities are shown in Figure 3.

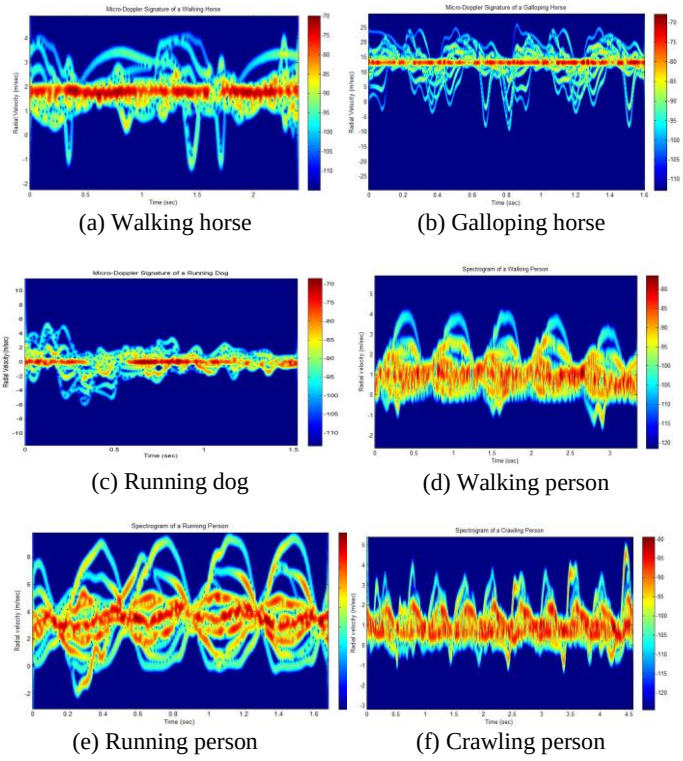

(a) Walking horse (b) Galloping horse

(c) Running dog (d) Walking person

(e) Running person (f) Crawling person

Figure 3. Example spectrograms for horses, dogs, and humans.

B. *Classification Performance Limitations*

An abundance of work has been published in the literature on the classification of micro-Doppler signatures. Under more or less ideal conditions, many works report achieving over 90% correct classification of human activities. For example, Kim and Ling [19] report a correct classification of about 92% using six features to classify seven different activities: running, walking, walking while holding a stick, crawling, boxing while moving forward, boxing while standing in place, and sitting still. Many different classifiers have been utilized, included but not limited to support vector machines, k-nearest neighbors, linear discriminant analysis, Gaussian mixture models, and artificial neural networks.

Moreover, literally dozens of features have been proposed, such as

- Physical features: e.g., *average torso Doppler frequency, bandwidth of torso oscillation, maximum of upper envelope, minimum of lower envelope, total Doppler bandwidth, average of upper envelope, average of lower envelope, difference between envelope averages, mean of envelope averages and, mean of envelope's maximum and minimum.*

- Speech-processing inspired features: *cepstral coefficients, mel-frequency cepstral coefficients, linear predictive coding coefficients*

- Cadence velocity diagram (CVD) features: *appendage-to-torso ratio, stride rate, and harmonic frequencies.*

However, under non-ideal conditions, despite the plethora of features, correct classification rates can drop to as lows 40% in the case when the target walks tangential to the antenna line-of-sight [20]. In fact, the operational conditions of the radar may have a drastic effect on classification performance. Two critical factors are SNR and dwell time.

In past work [7], it has been seen that dwell times of at least 2 seconds have been sufficient to attain high classification performance (>90%). For the TAN100 observing a target in stripmap mode, the total time-on-target attained when flying at 25 m/s may be found to be 6 seconds. Thus, for this airborne application, dwell time is not a limitation to classification.

SNR, however, is a limiting factor. Figure 4 shows the variations of normalized feature estimates with SNR. A subset of 6 physical features is shown in the figure, just for example. Notice that feature estimates begin to sharply deviate from their high SNR values at about 10-15 dB. At lower SNR values, classification performance will drop due to the degradation in estimation accuracy. At the minimum detection ranges computed in the previous section an SNR of 13 dB was attained. Thus, at the detected range the system should be able to accomplish classification for target recognition, although specific classification performance rates will be dependent upon the site-specific clutter levels and target classes involved.

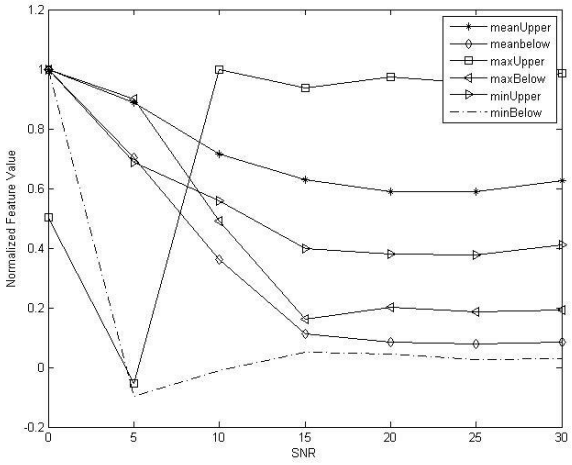

Figure 4. Variation of normalized feature values with SNR.

V. CONCLUSION

In this work, the system-level design considerations for a light-weight SAR mounted upon a short-range UAV geared towards human detection and classification missions was presented. It was found that the 2 lb nanoSAR could be mounted upon the TAN100 aircraft to detect humans at 850 meters, a range at which correct classification rates of above 90% may also be obtained for human activity recognition applications. The key design constraint upon the range is the tradeoff between transmit power and weight. As future work, performance improvements achievable by radar hardware modifications yielding higher transmit power, aircraft modifications permitting greater payload, and use of a phased-array antenna to permit multi-channel processing for clutter cancellation will be investigated.

ACKNOWLEDGEMENTS

The authors would like to acknowledge to contributions of Cesur Karabacak in simulating micro-Doppler signatures. This work was supported in part by TUBITAK Kariyer Project No. 113E105.

REFERENCES

[1] V. C. Chen, F. Li, S.-S. Ho, ve H. Wechsler, "Micro-Doppler effect in radar: phenomenon, model, and simulation study", *IEEE Trans. Aerosp. Electron. Syst.*, Vol. 42, No. 1, pp 2–21, 2006.

[2] V.C.Chen, *The Micro-Doppler Effect in Radar*. Artech House, 2010.

[3] Y. Kim ve H. Ling, "Human Activity Classification Based on Micro-Doppler Signatures Using a Support Vector Machine", *IEEE Trans. Geosci. Remote Sens.*, Vol. 47, No. 5, pp. 1328–1337, 2009.

[4] G. Greneker III, "Very low cost stand-off suicide bomber detection system using human gait analysis to screen potential bomb carrying individuals", 2005, Vol. 5788, pp. 46–56.

[5] M. Otero, "Application of a continuous wave radar for human gait recognition", 2005, Vol. 5809, pp. 538–548.

[6] D. Tahmoush ve J. Silvious, "Remote detection of humans and animals", *2009 IEEE Applied Imagery Pattern Recognition Workshop (AIPRW)*, 2009, pp. 1–8.

[7] Karabacak, C, Gurbuz, S.Z., Gurbuz, A,C, "Automatic human activity classification using radar," 22nd *Signal Processing and Communications Applications Conference (SIU)*, April 2014.

[8] http://www.imsar.com/products/display/2064/0/nanosar-c

[9] Öcal, F., Akçay, A., Ardıç, S., Kaynak, Ü., "Güneş Enerjili İnsansız Hava Aracı Tasarımı ve Geliştirilmesi", SAVTEK2012, 6. Savunma Teknolojileri Kongresi, 20-22 Haziran 2012, Ankara, Turkey.

[10] Barnard, J. "Unmanned Aircraft in Border Patrol Activities" Annual UAS Conference – Operational and Technology Readiness, 25– 26 September 2011.

[11] Richards, M., Fundamentals of Radar Signal Processing, McGraw Hill, New York, 2005.

[12] Ram, S.S.; Hao Ling, "Simulation of human microDopplers using computer animation data," *Radar Conference, 2008. RADAR '08. IEEE* , vol., no., pp.1,6, 26-30 May 2008.

[13] Van Dorp, P.,and F. C. A. Groen. "Human walking estimation with radar." *IEE Proceedings-Radar, Sonar and Navigation* 150.5 (2003): 356-365.

[14] B. Erol, C. Karabacak, S.Z. Gurbuz, "Simulation of human micro-Doppler signatures with Kinect sensor," in Proc. IEEE Radar Conference, Cincinatti, USA, 18-23 May 2014.

[15] http://mrl.snu.ac.kr/~mdb/session/

[16] http://accad.osu.edu/research/mocap/mocap_data.htm

[17] http://mocap.cs.cmu.edu/

[18] http://motion.cs.bilkent.edu.tr/

[19] Y. Kim and H. Ling, "Human activity classification based on micro-Doppler signatures Using a Support Vector Machine", *IEEE Trans. Geosci. Remote Sens.*, Vol. 47, No. 5, pp. 1328–1337, 2009.

[20] Tahmoush, D., Silvious, J., "Radar micro-doppler for long range front-view gait recognition," *IEEE 3rd Int. Conf. on Biometrics: Theory, Applications, and Systems*, pp.1,6, 28-30 Sept. 2009.